Int J Clin Exp Pathol 2014;7(9):5415-5428
www.ijcep.com /ISSN:1936-2625/IJCEP0001077

Original Article

Triggering the succinate receptor GPR91 enhances pressure overload-induced right ventricular hypertrophy

Lei Yang[1*], Di Yu[1*], Huan-Huan Fan[2*], Yu Feng[1], Liang Hu[1], Wei-Yan Zhang[1], Kai Zhou[1], Xu-Ming Mo[1]

[1]*Department of Cardiothoracic Surgery, Nanjing Children's Hospital Affiliated of Nanjing Medical University, Jiangsu Province, China;* [2]*Department of Gynaecology, Jiangsu Province Hospital of TCM, Jiangsu Province, China.* [*]*Equal contributors.*

Received June 11, 2014; Accepted June 26, 2014; Epub August 15, 2014; Published September 1, 2014

Abstract: Background: Pulmonary arterial hypertension (PAH) leads to pressure overload in the right ventricle (RV) and induces right ventricular hypertrophy (RVH). GPR91 is an orphan G-protein-coupled receptor (GPCR) that has been characterized as a receptor for succinate, which increases in RVH; however, its role remains unknown. Methods and results: We studied succinate-GPR91 signaling in a pulmonary arterial banding (PAB) model of RVH in the SD rats due to pressure overload. We report that GPR91 was located in cardiomyocytes. We found that the expressions of GPR91 and p-Akt in the RV significantly increased in the PAB model compared with the sham. In the PAB rats, the treatment of succinate further increased the p-Akt levels and aggravated RVH *in vivo*. In *in vitro* studies, succinate stimulated the up-regulation of the hypertrophic gene marker *anp*. All these effects were inhibited by the antagonist of PI3K, wortmannin, both *in vivo* and *in vitro*. Finally, we found that the GPR91-PI3K/Akt axis was also up-regulated compared with the sham in human RVH. Conclusions: Our results suggest that succinate-GPR91 is involved in RVH via PI3K/Akt signaling *in vivo* and *in vitro*. GPR91 may be a novel therapeutic target for RVH induced by pressure overload.

Keywords: Succinate G-protein-receptor 91, PI3K/Akt, right ventricular hypertrophy

Introduction

Right ventricular hypertrophy (RVH) is a major determinant of the prognosis in patients with pulmonary artery hypertension (PAH) [1-3]. RVH is characterized by increases in cell size and ventricle wall thickness, myofibrillar re-organization and re-expression of fetal genes, such as atrial natriuretic peptide (*anp*), eventually resulting in right heart failure (HF), and a leading cause of mortality worldwide [4-7]. The right ventricle (RV) has a half-moon shape (not ellipsoidal) and functions in a state of low pressure and high flow, pumping blood to the pulmonary vascular bed at a high capacitance [8]. These characteristics make the structure and function of the RV as well as the behavior and phenotypic patterns it can adopt under different stress situations different from those of the LV [9].

Succinate is an important metabolic molecule that constitutes one of the intermediates of the citric acid cycle. It is synthesized in the mitochondria by the oxidation of succinyl-CoA and is itself converted to fumarate by succinate dehydrogenase [10]. In addition to its conventional role in energy metabolism, other functions for this intermediate have been reported. Previous studies have reported that succinate stabilizes the transcription factor hypoxia-inducible factor-1α (HIF-1α) in specific tumors and in activated macrophages and that it stimulates dendritic cells [11, 12]. Furthermore, succinate has been shown to post-translationally modify proteins [13]. This expanding repertoire of functions for succinate suggests a broader role in cellular activation. Succinate has also been reported to be increased in the pressure-overloaded RV: under pressure overload conditions, the RV

augments the coronary flow to meet the increasing oxygen requirements. However, RV lower oxygen extractions reserve ultimately makes it less efficient at oxygen utilization despite the higher demand, and succinate accumulates under conditions linked to an insufficient oxygen supply [14].

A member of the G-protein-coupled receptor (GPCR) family, G-protein-receptor 91 (GPR91) has been shown to function as a receptor for succinate. A previous study has reported that in the kidneys, the principal signaling actions of succinate that are mediated by GPR91 are to increase Ca^{2+} via Gq and to decrease cAMP via Gi; the principal downstream effect that has been identified for these actions is an increase in renin release, which produces a rise in arterial blood pressure [15]. Recently, one study reported that GPR91 was expressed in rat ventricular cardiomyocytes and that Ca^{2+} transient and apoptosis were increased by succinate treatment and were also involved in cardiac hypertrophy [16]. Here, we fully substantiate a role for succinate and its cognate receptor, GPR91, in RVH caused by pressure overload.

In this study, we showed a previously undescribed function for succinate and its receptor GPR91 by establishing that RVH was caused by pressure overload via PI3K/Akt signaling. Our findings introduce a new paradigm of signaling with metabolic intermediates and establish the possibility of other yet unexplored metabolite signaling pathways.

Materials and methods

All procedures were followed by the recommendations of the ARRIVE guidelines of Animal Research: Reporting *in Vivo* Experiments (J Physiol. 2010) and were approved by the ethics committee of Nanjing Medical University.

Pulmonary artery banding (PAB) model establishment

All experimental protocols and surgical procedures used in this study were approved by the Institutional Animal Care and Use Committee of Nanjing Medical University. Surgical banding of the pulmonary artery was performed in male rats as described previously [17]. Via a left thoracotomy in rats weighing 180-200 g, a silk suture was tied tightly around an 18-gauge needle alongside the pulmonary artery. After the subsequent rapid removal of the needle, a fixed constricted opening was created in the lumen equal to the diameter of the needle. Whereas the initial constriction was relatively mild, the combination of the fixed banding around the pulmonary artery and the animal's growth resulted in a progressive increase in RV systolic pressure and a pressure gradient of approximately 60 mmHg after 6 weeks, as reported previously by others [18, 19]. In the sham group, all the rats have received the same procedure except the silk suture fixed constriction.

Succinate concentration in this article

Succinate has been reported to stimulate multilineage blood cell recovery from chemotherapy-induced myelosuppression at a concentration of 30 mg/kg/day [10]. In our preliminary experiment, we selected three succinate concentrations: 30 mg/kg/day, 50 mg/kg/day and 100 mg/kg/day. The rats were are sacrificed by over-volume midazolam and chloral hydrate when they displayed low body weight and limb edema caused by the right heart failure. At the conclusion of the experiment, we found that the 30 mg/kg/day group experienced less significant RVH than the 50 mg/kg/day group (**Appendix Figure 1A**). Moreover, all the rats except one in the 100 mg/kg/day group died before the end of the experiment (**Appendix Figure 1B**). Finally, the 50 mg/kg/day concentration was selected for the formal animal experiment. For the *in vitro* study, we selected the two succinate concentrations of 5 mM and 10 mM, according to reports by others [10]. Because the succinate concentration of 10 mM showed higher expression levels of *anp* in the cardiomyocytes (**Appendix Figure 1C**), we selected it for the formal concentration in the *in vitro* experiments.

Pressure and right ventricular hypertrophy measurements

Invasive pressure measurements of right ventricular systolic pressure (RVSP) were performed as described previously [20]. After anesthesia, the rats' tracheas were orally intubated with a 16-gauge intravenous catheter, and mechanical ventilation was commenced using a rodent respirator (tidal volume: 8 ml/kg, respiratory rate: 60/min). The pressure parameters were measured by direct puncture

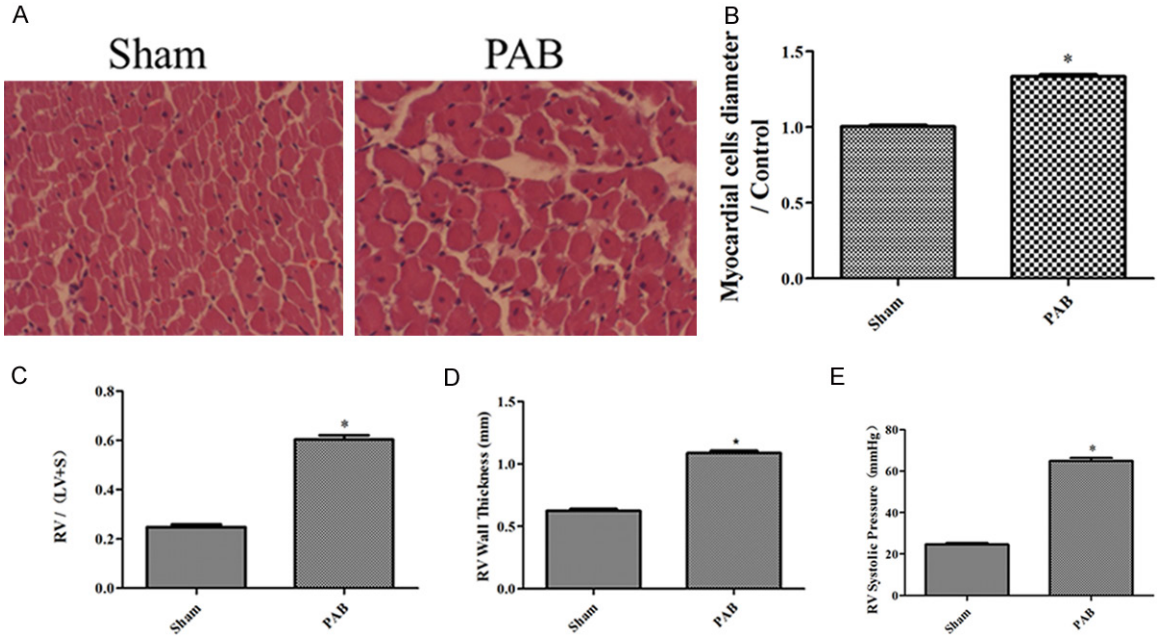

Figure 1. The PAB model establishment. A: Representative images of HE-stained RV sections from the sham, PAB rats; B: The myocardial cells diameter/Control in the sham, PAB rats (n=6); C: RV hypertrophy indexed by the ratio of the wet weight of the RV to the left ventricular wall plus the septum [RV/(LV+S)] in the sham, PAB (n=3); D: The thickness of the RV in the sham, PAB rats (n=3); E: RV systolic pressure of the sham, PAB rats (n=8); *$P < 0.05$, compared with the sham.

of the RV followed by advancement of the catheter into the RV (which was confirmed by a standard right ventricle pressure trace on the monitor screen), which was then connected to the pressure transducer of a BSM-1700 monitor (Nihon Kohden Company, Japan). The data for the right ventricle systolic pressure (RVSP) were recorded after 1 minute of stabilization. After the measurements are finished, all rats are sacrificed by over-volume midazolam and chloral hydrate. After the rats' death, the hearts are harvested and the RV free wall was dissected from the left ventricle plus the septum (LV+S) and weighed separately; the RV hypertrophy was expressed as RV/ (LV+S). During all the procedure, the rats were analgesia and unconscious.

Histological analysis

The hearts were excised, washed with saline solution and placed in 10% formalin. Several sections of the hearts (4-5 μm thick) were prepared and stained with hematoxylin and eosin (HE) for histopathology and then visualized by light microscopy.

Evaluation of RVH

RVH was evaluated as described previously [21]. To determine the degree of RVH, RV tissue sections were stained with HE. The diameters of 20 myocardial cells were measured per tissue section by Image-Pro Plus 6.0 (Media Cybernetics, USA). RVH degree=the diameter/ the average sham diameter. All the diameters in one group averaged and the mean diameter of each group is taken as the final result.

Immunofluorescence

Immunofluorescence staining was performed using primary antibodies to detect GPR91 (1:50; Novus, USA) and alpha actinin (1:50; Abcam, USA), followed by incubation in a fluorescein isothiocyanate-conjugated secondary antibody (1:100; Bioworld, China). For the negative sham experiments, the primary antibodies were omitted.

Western blotting

The specimens were homogenized using a tissue homogenizer or lysed in RIPA buffer (Bi Yun-

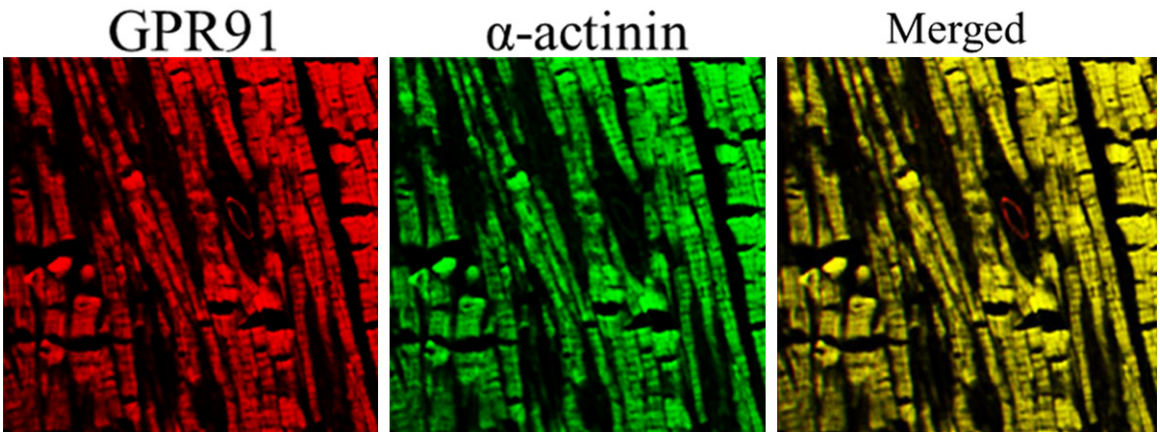

Figure 2. Expression and distribution of GPR91 in the heart. Confocal immunofluorescent images of the rat heart show that staining for GPR91 (red) and the cardiomyocyte marker actinin (green) co-localize (merged).

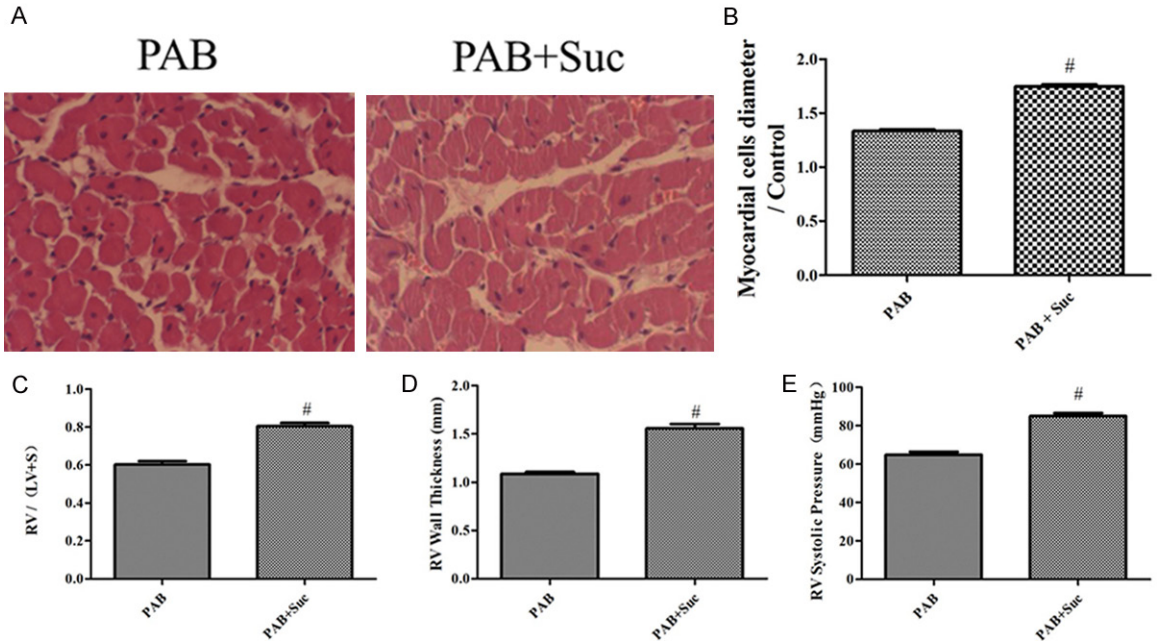

Figure 3. Succinate accelerated RVH in the PAB model. A: Representative images of HE-stained RV sections from the PAB, PAB+Suc rats; B: The myocardial cells diameter/Control in the PAB, PAB+Suc rats (n=8); C: RV hypertrophy indexed by the ratio of the wet weight of the RV to the left ventricular wall plus the septum [RV/(LV+S)] in the PAB, PAB+Suc (n=8); D: The thickness of the RV in the PAB, PAB+Suc rats (n=8); E: RV systolic pressure of the PAB, PAB+Suc rats (n=8); $^{\#}P < 0.05$, compared with the PAB.

tian, China) with the addition of a protease inhibitor cocktail (Bi Yun-tian, China) and PMSF. Tissue lysates were equalized with SDS 5× sample buffer, electrophoretically separated on 10% polyacrylamide gels and transferred for 1 h onto nitrocellulose membranes. Subse quently, the membranes were blocked for 1 h with 5% non-fat dry milk in Tris buffered saline/0.1% Tween 20. After blocking, the membranes were probed with primary antibodies diluted as follows: GPR91 (1:1000; Novus, USA), Akt (1:1000; Sigma, USA), p-Akt (1:1000; Sigma, USA) and Tubulin (1:5000, Bi Yun-tian, China). After primary antibody incubation, the membranes were incubated with secondary goat anti-rabbit (1:10000, Bi Yun-tian, China) or rabbit anti-goat (1:10000, Bi Yun-tian, China) HRP-conjugated antibodies (ZSGB-BIO). Signals

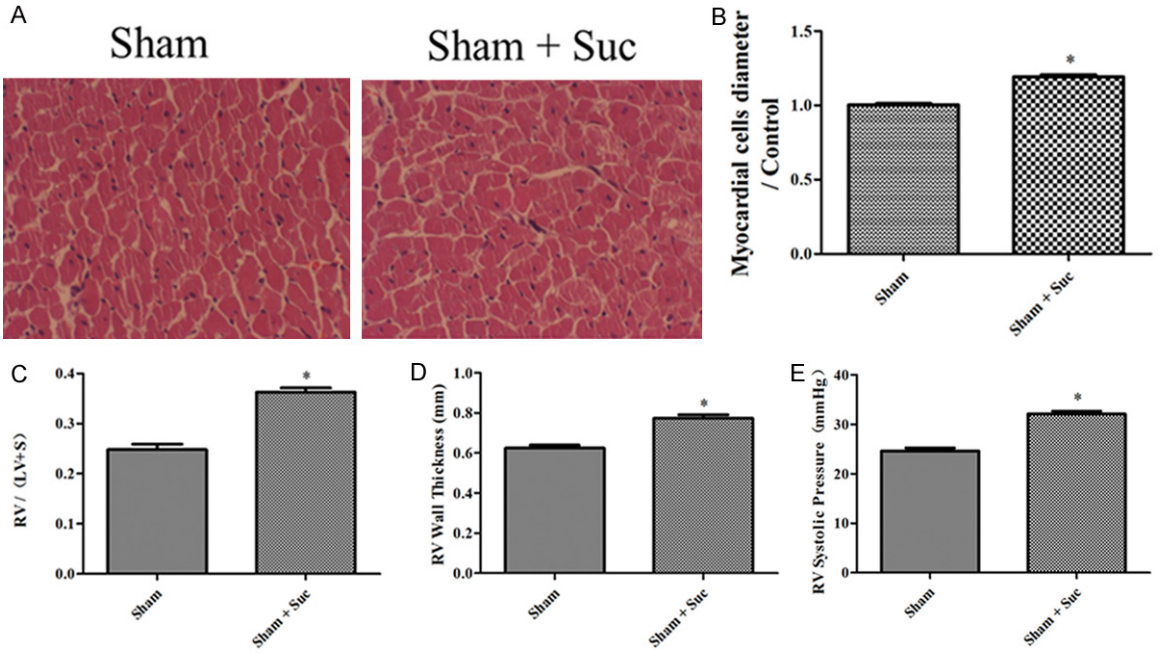

Figure 4. Succinate caused RVH in the sham group. A: Representative images of HE-stained RV sections from the sham, sham+Suc rats; B: the myocardial cells diameter/Control in the sham, sham+Suc rats (n=8); C: RV hypertrophy indexed by the ratio of the wet weight of the RV to the left ventricular wall plus the septum [RV/(LV+S)] in the sham, sham+Suc (n=8); D: The thickness of the RV in the sham, sham+Suc rats (n=8); E: RV systolic pressure of the sham, sham+Suc rats (n=8); *$^*P < 0.05$, compared with the sham.

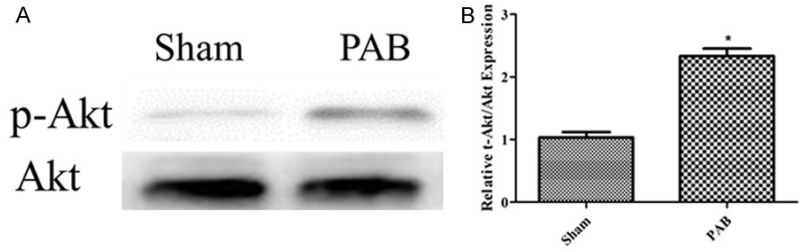

Figure 5. Up-regulation of PI3K/Akt signaling in RVH. A: p-Akt/Akt expression from the western blotting image of the sham, PAB; B: The bar graph shows the p-Akt/Akt expression from the western blotting images of the sham, PAB (n=3); *$^*P < 0.05$, compared with the sham.

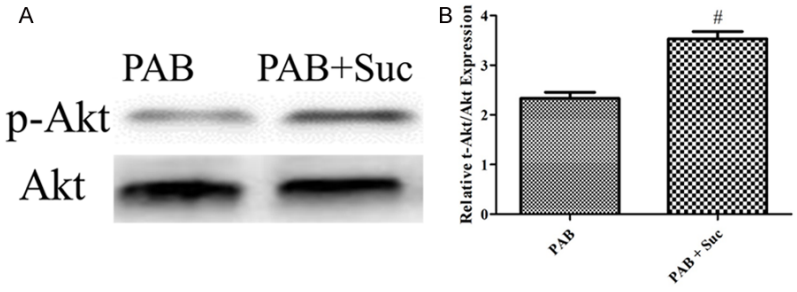

Figure 6. Succinate elicits further activation of PI3K/Akt signaling in RVH. A: p-Akt/Akt expression from the western blotting image of the PAB, PAB+Suc; B: The bar graph shows the p-Akt/Akt expression from the western blotting images of the PAB, PAB + Suc (n=3); #$P < 0.05$, compared with the PAB.

were then detected by the ECL detection system (BIO-RAD, USA) and further quantified using Image J software (National Institutes of Health, USA).

Real-time quantitative polymerase chain reaction

Total RNA of the right ventricle was extracted with the TRIzol reagent (Invitrogen, USA) according to the manufacturer's instructions. Reverse transcription was then performed using 1 μg of total RNA with the Transcriptor First Strand cDNA Synthesis Kit (Roche, Germany). A real-time quantitative polymerase chain reaction (QPCR) was conducted using ABI PRISM® 7500 QPCR System according to the manufacturer's guidelines. Two-step QPCR was used to perform the relative quantifi-

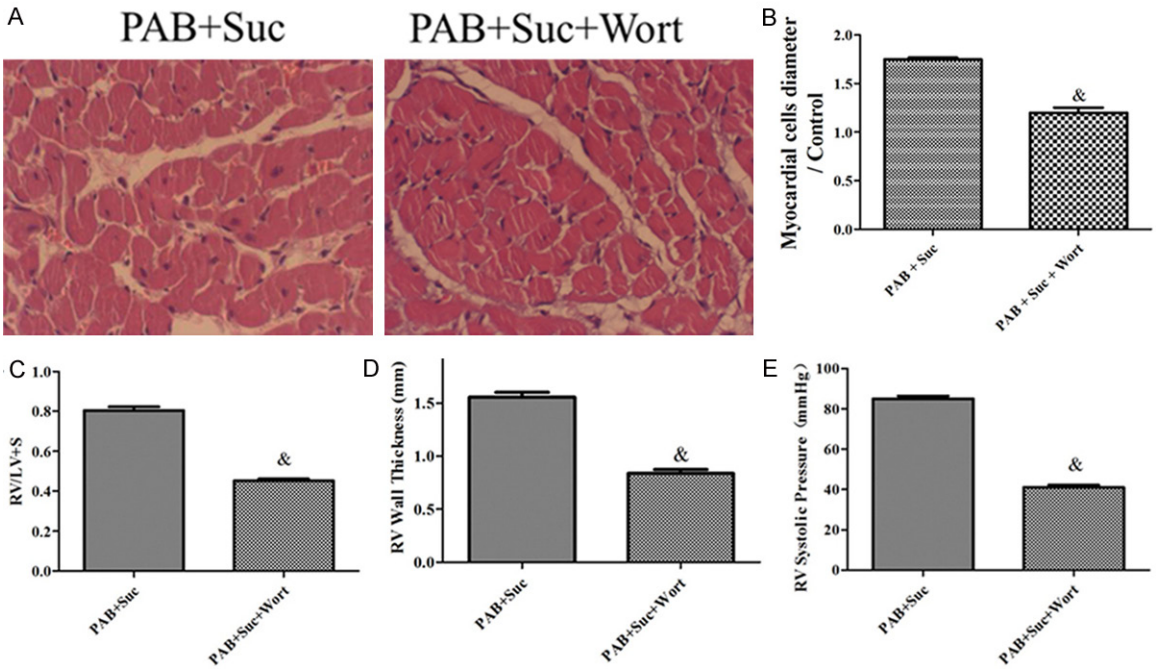

Figure 7. Wortmannin inhibits severe RVH elicited by succinate. A: Representative images of HE-stained RV sections from the PAB+Suc, PAB+Suc+Wort rats; B: The myocardial cells diameter/Control in the PAB+Suc, PAB+Suc+Wort rats (n=8); C: RV hypertrophy indexed by the ratio of the wet weight of the RV to the left ventricular wall plus the septum [RV/(LV+S)] in the PAB+Suc, PAB+Suc+Wort (n=8); D: The thickness of the RV in the PAB+Suc, PAB+Suc+Wort rats (n=8); E: RV systolic pressure of the PAB+Suc, PAB+Suc+Wort rats (n=8); *&P < 0.05,* compared with the PAB+Suc.

cation of mRNA. Glyceraldehyde-3phosphate dehydrogenase (GAPDH) was selected as an internal housekeeping gene sham for the comparative Ct method for the relative quantification of the mRNA expression of target genes. The fluorescent product was detected at the end of each cycle. The products' specificity was confirmed by agarose gel electrophoresis and a routine melting-curve analysis. The primers were designed as described by Paulo Renato A.V. Correa using the software Primer3 based on the sequence deposited in the NCBI Nucleotide Bank. The data were analyzed with the ABI Prism 7500 sequence detection system software (version 1.4), and GAPDH was used as an internal sham for input RNA.

Cultured neonatal rat cardiomyocytes

Primary cultures of the cardiomyocytes were prepared as described previously [22]. Cells from the hearts of 1-day-old Sprague-Dawley rats were seeded at a density of 1×10^6/well onto 6-well culture plates. The cells were kept quiescent for 48 hours, and then the medium was changed to either 10% FBS (Invitrogen, USA)/DMEM (Invitrogen, USA)/BrdU (Bi Yuntian, China) alone or with the addition of succinate or of succinate plus wortmannin.

Small interfering RNA (siRNA) transfection

Rat GPR91 (NC_005101.3) siRNAs were synthesized by Gene Pharma (Shanghai, China). The primer sequences for siRNA synthesis are the following: 5'-AATCTCTAATGCCAGCCAAT CCTGTCTC-3' (sense) and 5'-AAAATTGGCTGG CATTAGAGACCTGTCTC-3' (antisense) for rat GPR91. Non-targeting (scrambled sequence) fluorescein isothiocyanate (FITC)-conjugated -siRNA was used as negative control to discriminate nonspecific effects. FITC-conjugated -siRNAs were transfected into cardiomyocytes with siRNA-Mate™ reagent (Gene Pharma, Shanghai, China) at a final concentration of 5 nM siRNA for cardiomyocytes at 2 ml/well in 6-well plates. The efficiency of the transfection was estimated by fluorescent microscopy (Olympus, Japan). The mRNA knockdown was confirmed by RT-qPCR 48 h after transfection. Protein level was confirmed by western-blotting 72 h after transfection (**Appendix Figure 2**).

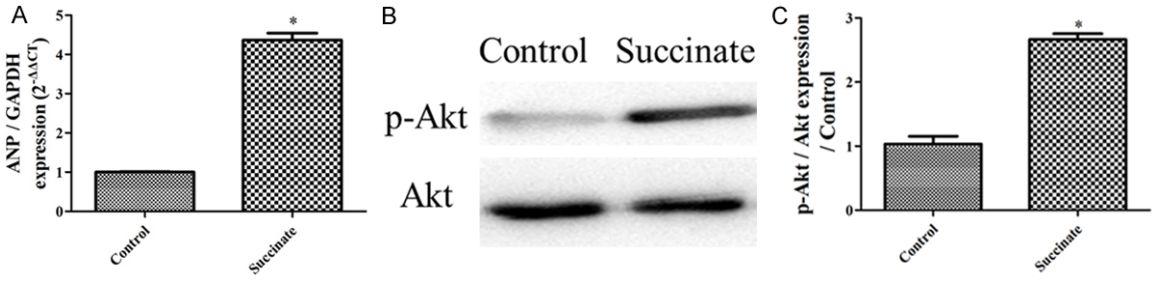

Figure 8. Succinate caused the activation of RVH gene and PI3K/Akt signaling in the cardiac muscle cell *in vitro*. A: ANP gene expression in the control, succinate group (n=3); B: p-Akt/Akt expression in the control, succinate group; C: The bar graph shows the p-Akt/Akt expression from the western blotting images (n=3); *$^{*}P < 0.05$, compared with the control.

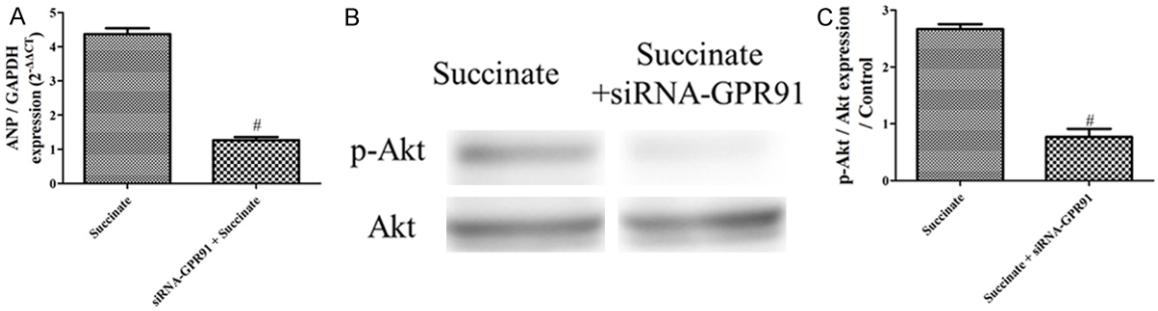

Figure 9. siRNA-GPR91 inhibits activation of RVH gene and PI3K/Akt signaling elicited by succinate *in vitro.* A: ANP gene expression in the control, succinate group (n=3); B: p-Akt/Akt expression in the control, succinate group (n=3); C: The bar graph shows the p-Akt/Akt expression from the western blotting images (n=3); $^{\#}P < 0.05$, compared with the succinate.

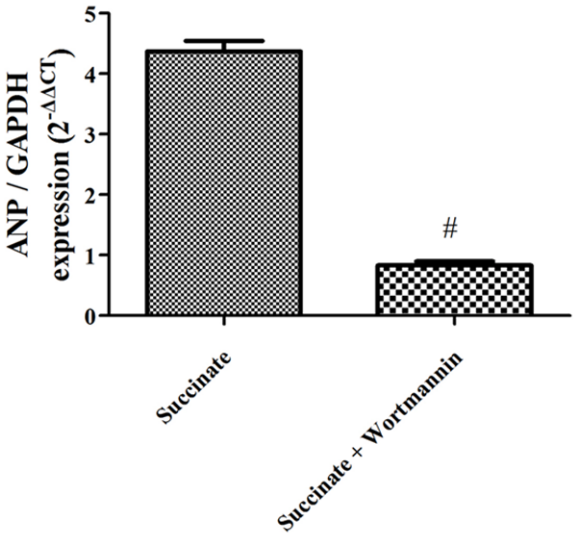

Figure 10. Wortmannin inhibits the activation of RVH gene elicited by succinate *in vitro.* ANP gene expression in the succinate, succinate + wortmannin group (n=3).

Statistical analysis

The data are presented as the mean±SEM. Statistical analyses were performed using the IBM SPSS Statistics 19 statistical software program. The means among groups were compared using one-way ANOVA, followed by Student-Newman-Keuls's post hoc test. Statistical significance was set at $P < 0.05$.

Results

RVH establishment in PAB rats

In our study, we used PAB animal models for RVH. HE staining and histological analysis showed a significant increase in the size of the RV cardiomyocytes in the PAB rats compared with the shams (**Figure 1A** and **1B**). We have also found that PAB rats develop significant increases in RV/(LV+S), RVWT and RVSP compared with the shams (**Figure 1C-E**).

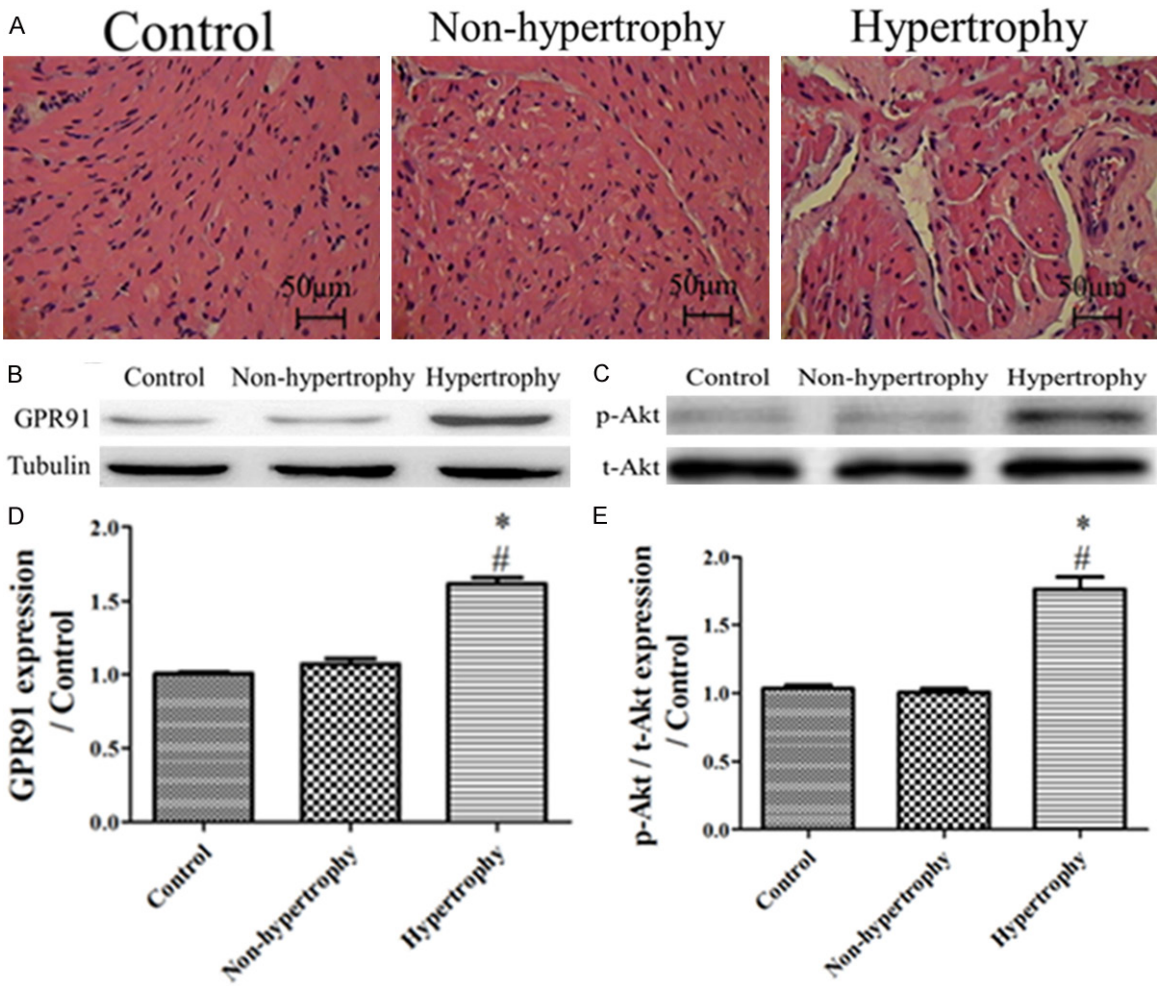

Figure 11. GPR91-PI3K/Akt signaling also exists in the human heart. A: Representative images of HE-stained RA sections from sham, hypertrophic and non-hypertrophic humans; B: GPR91 expression of the Western-blotting image from the RA of sham, hypertrophic and non-hypertrophic patients; C: p-Akt/Akt expression from the RA of sham, hypertrophic and non-hypertrophic patients; D: Bar graph showing the GPR91 expression of the Western-blotting images from the RA of sham, hypertrophic and non-hypertrophic patients, respectively (n=3); E: Bar graph showing the p-Akt/Akt expression of the Western-blotting images from the RA of sham, hypertrophic and non-hypertrophic patients, respectively (n=3); *$^{*}P < 0.05$, compared with the sham; $^{\#}P < 0.05$, compared with the non-hypertrophic patients.

Expression and distribution of GPR91 in the heart

To assess whether GPR91 may have a role in RVH, we determined the localization of GPR91 in the heart. The staining of RV sections with a GPR91 antibody followed by confocal laser scanning microscopy clearly showed that GPR91 was strongly expressed in and localized to the RV cardiomyocytes, indicating that GPR91 participates in RV function (**Figure 2**).

Succinate accelerated RVH in the PAB model

We postulated that the administration of succinate, an agonist of GPR91, could further accelerate RVH in the PAB model. The HE staining and histological analysis demonstrated a strong RVH response, as shown by myocardial fiber thickening, nuclear deformation and uneven dyeing in the RV, after the administration of succinate compared with the placebo given to the PAB rats (**Figure 3A** and **3B**). Furthermore, succinate administration in the PAB rats significantly increased RV/(LV+S), RVWT and RVSP compared with the placebo (**Figure 3C-E**).

Succinate caused RVH in the sham group

The HE staining and histological analysis demonstrated a significant RVH response after the

administration of succinate in the sham rats compared with the placebo given to the sham rats (**Figure 4A** and **4B**). Furthermore, succinate administration in the sham rats significantly increased RV/(LV+S), RVWT and RVSP compared with the placebo (**Figure 4C-E**).

Up-regulation of PI3K/Akt signaling in RVH

To assess the activity of PI3K/Akt signaling in RVH, we determined the p-Akt/Akt expression as a representative of the activation of PI3K/Akt signaling. The protein expression level of p-Akt/Akt was significantly increased in the RVH group compared with the sham (**Figure 5**).

Succinate elicits further activation of PI3K/Akt signaling in RVH

We found that after the administration of succinate, the p-Akt/Akt was further increased in the RV in the PAB group after succinate administration compared with the placebo (**Figure 6**).

Wortmannin inhibits severe RVH elicited by succinate

The HE staining and histological analysis demonstrated that wortmannin inhibited myocardial fiber thickening, nuclear deformation and the uneven dyeing in the RV in the PAB elicited by succinate (**Figure 7A** and **7B**). After the wortmannin administration to the succinate groups, the elevations of RV/(LV+S), RVWT and RVSP elicited by succinate in the PAB models were also found to be significantly inhibited (**Figure 7C-E**).

Succinate caused the activation of RVH gene and PI3K/Akt signaling in the cardiac muscle cell in vitro

Exposure of the cells to succinate led to the up-regulation of RVH gene *anp* expression levels compared with the control (**Figure 8A**). Furthermore, exposure of the cells to succinate led to the increase of p-Akt/Akt compared with the control (**Figure 8B** and **8C**).

siRNA-GPR91 inhibits activation of RVH gene and PI3K/Akt signaling elicited by succinate in vitro

siRNA-GPR91 inhibits the up-regulation of RVH gene *anp* expression levels compared with the group succinate (**Figure 9A**). Furthermore, siRNA-GPR91 inhibits the increase of p-Akt/Akt compared with the group succinate (**Figure 9B** and **9C**).

Wortmannin inhibits the inhibits activation of RVH gene elicited by succinate in vitro

Wortmannin inhibits the up-regulation of RVH gene *anp* expression level elicited by succinate compared with the group succinate (**Figure 10**).

GPR91-PI3K/Akt signaling also exists in humans

To determine whether the GPR91-PI3K/Akt axis could be involved in cardiac hypertrophy in humans, we performed western blotting on the right atrium in sham, hypertrophic and non-hypertrophic patients. We also analyzed histological sections by HE staining to confirm cardiac hypertrophy. As expected, the GPR91-PI3K/Akt axis showed a significant increase in hypertrophic patients (**Figure 11**) compared with the non-hypertrophic and sham patients. There were no significant differences in the protein expression levels between the sham and non-hypertrophic patients.

Discussion

Although succinate has been intensely studied for more than 60 years in the context of energy production, the recent demonstration that it can induce cellular signaling transduction through GPR91 has raised the possibility of physiological properties beyond its traditional role as a Krebs cycle metabolite [23]. In the present study, we found that the succinate-GPR91-PI3K/Akt axis exists in RVH in response to pressure overload *in vivo* and *in vitro*. The effects of succinate can be mitigated by the down-regulate of GPR91 and the wortmannin, an inhibitor of Akt, *in vivo* and *in vitro*, indicating that the PI3K/Akt axis is downstream of succinate-GPR91 in RVH. We also found that the succinate-GPR91-PI3K/Akt axis exists in the human heart. As a whole, our data showed that succinate-GPR91 was involved in RVH induced by pressure overload via the PI3K/Akt pathway.

PAH is a severe complication in which vasoconstriction and vascular remodeling both lead to a progressive increase in pulmonary vascular resistance [24, 25]. The response of the RV to the increased pressure load is an important

determinant of the outcome PAH patients [26]. Pressure overload imposes a hemodynamic burden on the RV, which, in turn, initiates a series of events leading to RV remodeling, RVH and eventually HF, which is closely associated with poor outcomes [27-29]. Although RVH secondary to RV outflow track in obstruction (RVOTO) can occasionally be compensatory to enhance contractility and preserve RV function, RVH is still characterized by ventricular remodeling associated with increases in both fibrosis and cardiomyocyte size, resulting in the enlargement of the heart and depressed contractile function, thereby increasing long-term mortality [9, 30-32]. The RV is derived embryologically from different heart fields than the LV and manifests differences in calcium handling, inotropy and gene expression patterns in response to stress. Consequently, the standard treatments for LV hypertrophy (ACE inhibitors, β-blockers) have shown limited success in RVH [33-35].

In 2004, combining the mass spectrometry results with the biochemical properties of the ligand, the purified GPR91 ligand was confirmed to be succinate [15]. Succinate is a well-known intermediate in the tricarboxylic acid (Krebs) cycle, and formed from succinyl-CoA by succinyl-CoA synthetase and subsequently converted by succinate dehydrogenase to generate fumarate [36]. This research implied a signaling role for succinate beyond energy production and established a direct link between the metabolic system and the cell signal transduction system. In the kidney, succinate is reported to regulate the renin-angiotensin-aldosterone system and suggested to be important in the development of renovascular hypertension and diabetic nephropathy [15]. Succinate effect in neuronal retinal ganglion cells has been reported to have a pro-angiogenic effect involved in retinopathy of prematurity [23]. In a recombinant system expressing GPR91, succinate was confirmed to result in both 3'-5'-cyclic adenosine monophosphate (cAMP) inhibition and inositol phosphate formation in a pertussis toxin (PTX)-sensitive manner [36]. In healthy humans, the succinate serum concentration is generally approximately 5 μM; however, in response to pressure overload of the heart, circulating concentrations up to the millimolar range have been detected [37]. Therefore, succinate appears to be particularly important in the setting of pathological conditions in the pressure-overloaded heart. Here, we have fully substantiated a role for succinate in mediating RVH that occurs during pressure overload *in vivo* and *in vitro*. Moreover, we found that succinate-GPR91 signaling also exists in human RVH.

GPCRs are essential regulators of cellular physiology and pathophysiology, and mutations or modifications of members of this receptor family are associated with aberrant cellular signaling and disease [38, 39]. GPCRs have proven to be excellent targets for drug discovery, where approximately 40-50% of the therapeutics used to treat disease are thought to specifically target their actions [40, 41]. Moreover, a large subset of the GPCR family includes orphan receptors with no known agonists and may provide a potential source of novel therapeutic targets for the treatment of disease [42]. GPR91 has been found to be involved in regulating many important biological effects. For example, GPR91, as a regulator of various angiogenic factors including VEGF and angiopoietins, provides an alternative target to govern revascularization after ischemia in the retina [23]; the intravitreal injection of the small interfering RNA against GPR91 suppressed the angiogenic effects of succinate, verifying that succinate's effects were governed by GPR91 [23]. Furthermore, the intravenous injection of succinate into rats leads to hypertension; however, succinate was unable to induce hypertension in GPR91-deficient mice [15]. Recently, researchers have established that cardiomyocytes express GPR91 in the sarcolemmal membrane and found that succinate, through GPR91, increases the amplitude and rate of decline of global transient Ca^{2+} in this cell type by increasing the phosphorylation levels of the ryanodine receptor and phospholamban, two well-known Ca^{2+}-handling proteins [16]. Additionally, they found that succinate decreases cardiomyocyte apoptosis [16]. The transient Ca^{2+} and cardiomyocyte apoptosis are both important signals in cardiac hypertrophy [43, 44]. Taken together, we propose that succinate-GPR91 signaling could regulate RVH that is induced by pressure overload. As the Krebs cycle and the respiratory chain are ancestral processes that are intimately involved with energy production in cardiomyocytes, it is not surprising that cardiomyocytes exploit at least one metabolite, succinate,

as a crucial regulator of RVH induced by pressure overload.

The PI3K/Akt pathway has also been implicated in cardiac hypertrophy [45, 46]. In fact, experiments with adult rat cardiomyocytes have demonstrated that the activation of angiotensin receptor type 1 via the NADPH oxidase-2 pathway, which participates in the regulation of mitochondrial biogenesis and increases cardiac succinate levels, can stimulate cardiac hypertrophy *in vivo* and *in vitro*; this hypertrophic effect was shown to be mediated by PI3K/Akt [47]. The inhibition of NADPH oxidase is also known to significantly inhibit the PI3K/Akt pathway, decreasing cardiac hypertrophy, apoptosis, inflammation and ROS generation [48]. We found that treatment with an excessive succinate concentration accelerated RVH through a GPR91-PI3K/Akt-dependent pathway both *in vivo* and *in vitro*. Our findings indicate that PI3K/Akt is downstream of succinate-GPR91, which accelerates RVH. We report that the succinate-GPR91-PI3K/Akt axis also exists in the human heart. The PI3K/AKT pathway is well-known to be activated by Gi [49]. Therefore, the succinate-GPR91 pathway, through the Gi pathway, may activate PI3K/AKT. Further experiments need to be performed to investigate this possibility.

In conclusion, we have found that succinate-GPR91 plays a critical role in pressure overload-induced RVH *in vivo* and *in vitro*. We also indicated that the PI3K/Akt signaling pathway is involved in the effects of succinate-GPR91-mediated RVH. Our results provide a framework for future studies investigating the role of GPR91 in RVH.

Limitations

This study has several potential limitations. In our research, succinate-GPR91 has been confirmed to be involved in the RVH. Indeed, RVH has a close relationship with left ventricle hypertrophy (LVH), but we currently have no data showing whether these factors are involved in LVH. Further experiments are also needed to investigate this.

Acknowledgements

This work was supported by the National Nature Science Foundation of China (81370277) and the National 12th Five-Year technology based plan topic (2011BAI11B22) and was sponsored by the Research and Innovation Project for College Graduates of Jiangsu Province (CXLX-0560).

Disclosure of conflict of interest

None.

Address correspondence to: Dr. Xu-Ming Mo, Department of Cardiothoracic Surgery, Nanjing Children's Hospital Affiliated of Nanjing Medical University, Center of Children with Congenital Heart Disease of Jiangsu Province, 72 of Guangzhou Road, Nanjing 210008, P. R. China. E-mail: mohsuming15@sina.com

References

[1] Azakie A, Fineman J, He Y. Differential responses of the right ventricle to abnormal loading conditions in vivo: possible pathophysiologic mechanisms. J Thorac Cardiovasc Surg 2013; 145: 1335-1344.

[2] Meng L, Liu X, Zheng Z, Li J, Meng J, Wei Y, Hu S. Original rat model of high kinetic unilateral pulmonary hypertension surgically induced by combined surgery. J Thorac Cardiovasc Surg 2013; 146: 1220-1226.

[3] Nguyen R, Mir TS, Kluwe L, Jett K, Kentsch M, Mueller G, Kehrer-Sawatzki H, Friedman J, Mautner VF. Cardiac characterization of 16 patients with large NF1 gene deletions. Clin Genet 2013; 84: 344-349.

[4] Farmer DG, Ewart MA, Mair KM, Kennedy S. Soluble receptor for advanced glycation end products (sRAGE) attenuates haemodynamic changes to chronic ypoxia in the mouse. Pulm Pharmacol Ther 2014; [Epub ahead of print].

[5] Angeli E, Pace Napoleone C, Turci S, Oppido G, Gargiulo G. Pulmonary artery banding. Multimed Man Cardiothorac Surg 2012; 2012: mms010.

[6] Stuckey DJ, McSweeney SJ, Thin MZ, Habib J, Price AN, Fiedler LR, Gsell W, Prasad SK, Schneider MD. T_1 Mapping Detects Pharmacological Retardation of Diffuse Cardiac Fibrosis in Mouse Pressure-overload Hypertrophy. Circ Cardiovasc Imaging 2014; 7: 240-9.

[7] Dunlop K, Gosal K, Kantores C, Ivanovska J, Dhaliwal R, Desjardins JF, Connelly KA, Jain A, McNamara PJ, Jankov RP. Therapeutic hypercapnia prevents inhaled nitric oxide-induced right ventricular systolic dysfunction in juvenile rats. Free Radic Biol Med 2014; 69: 35-49.

[8] Bove T, Vandekerckhove K, Bouchez S, Wouters P, Somers P, Van Nooten G. Role of myocardial hypertrophy on acute and chronic right ven-

tricular performance in relation to chronic volume overload in a porcine model: Relevance for the surgical management of tetralogy of Fallot. J Thorac Cardiovasc Surg 2014; 147: 1956-65.
[9] J Sánchez-Lázaro I, Almenar Bonet L, Igual Muñoz B, Rueda-Soriano J, Martínez-Dolz L, Zorio-Grima E, Angel Arnau-Vives M, Salvador-Sanz A. Phenotypic patterns of right ventricular dysfunction: analysis by cardiac magnetic imaging. Heart Int 2013; 8: e3.
[10] Hakak Y, Lehmann-Bruinsma K, Phillips S, Le T, Liaw C, Connolly DT, Behan DP. The role of the GPR91 ligand succinate in hematopoiesis. J Leukoc Biol 2009; 85: 837-843.
[11] Pearce EL, Pearce EJ. Metabolic pathways in immune cell activation and quiescence. Immunity 2013; 38: 633-643.
[12] Mills E, O'Neill LA. Succinate: a metabolic signal in inflammation. Trends Cell Biol 2014; 24: 313-20.
[13] Tannahill GM, Curtis AM, Adamik J, Palsson-McDermott EM, McGettrick AF, Goel G, Frezza C, Bernard NJ, Kelly B, Foley NH, Zheng L, Gardet A, Tong Z, Jany SS, Corr SC, Haneklaus M, Caffrey BE, Pierce K, Walmsley S, Beasley FC, Cummins E, Nizet V, Whyte M, Taylor CT, Lin H, Masters SL, Gottlieb E, Kelly VP, Clish C, Auron PE, Xavier RJ, O'Neill LA. Succinate is an inflammatory signal that induces IL-1β through HIF-1α. Nature 2013; 496: 238-242.
[14] Dias CA, Assad RS, Caneo LF, Abduch MC, Aiello VD, Dias AR, Marcial MB, Oliveira SA. Reversible pulmonary trunk banding. II. An experimental model for rapid pulmonary ventricular hypertrophy. J Thorac Cardiovasc Surg 2002; 124: 999-1006.
[15] He W, Miao FJ, Lin DC, Schwandner RT, Wang Z, Gao J, Chen JL, Tian H, Ling L. Citric acid cycle intermediates as ligands for orphan G-protein-coupled receptors. Nature 2004; 429: 188-193.
[16] Aguiar CJ, Andrade VL, Gomes ER, Alves MN, Ladeira MS, Pinheiro AC, Gomes DA, Almeida AP, Goes AM, Resende RR, Guatimosim S, Leite MF. Succinate modulates Ca(2+) transient and cardiomyocyte viability through PKA-dependent pathway. Cell Calcium 2010; 47: 37-46.
[17] Chen YL, Su MC, Liu WH, Wang CC, Lin MC, Chen MC. Influence and Predicting Variables of Obstructive Sleep Apnea on Cardiac Function and Remodeling in Patients without Congestive Heart Failure. J Clin Sleep Med 2014; 10: 57-64.
[18] Novoyatleva T, Janssen W, Wietelmann A, Schermuly RT, Engel FB. TWEAK/Fn14 axis is a positive regulator of cardiac hypertrophy. Cytokine 2013; 64: 43-45.
[19] Borgdorff MA, Bartelds B, Dickinson MG, Steendijk P, Berger RM. A cornerstone of heart failure treatment is not effective in experimental right ventricular failure. Int J Cardiol 2013; 169: 183-189.
[20] Stastna M, Van Eyk JE. Optimized method for identification of the proteomes secreted by cardiac cells. Methods Mol Biol 2013; 1005: 225-235.
[21] Picatoste B, Ramirez E, Caro-Vadillo A, Iborra C, Ares-Carrasco S, Egido J, Tunon J, Lorenzo O. Sitagliptin reduces cardiac apoptosis, hypertrophy and fibrosis primarily by insulin-dependent mechanisms in experimental type-II diabetes. Potential roles of GLP-1 isoforms. PLoS One 2013; 8: e78330.
[22] Chiarini A, Micucci M, Malaguti M, Budriesi R, Ioan P, Lenzi M, Fimognari C, Gallina Toschi T, Comandini P, Hrelia S. Sweet chestnut (Castanea sativa Mill.) bark extract: cardiovascular activity and myocyte protection against oxidative damage. Oxid Med Cell Longev 2013; 2013: 471790.
[23] Sapieha P, Sirinyan M, Hamel D, Zaniolo K, Joyal JS, Cho JH, Honore JC, Kermorvant-Duchemin E, Varma DR, Tremblay S, Leduc M, Rihakova L, Hardy P, Klein WH, Mu X, Mamer O, Lachapelle P, Di Polo A, Beauséjour C, Andelfinger G, Mitchell G, Sennlaub F, Chemtob S. The succinate receptor GPR91 in neurons has a major role in retinal angiogenesis. Nat Med 2008; 14: 1067-1076.
[24] Kohler D, Arnold R, Loukanov T, Gorenflo M. Right Ventricular Failure and Pathobiology in Patients with Congenital Heart Disease-Implications for Long-Term Follow-Up. Front Pediatr 2013; 1: 37.
[25] McLaughlin VV, Gaine SP, Howard LS, Leuchte HH, Mathier MA, Mehta S, Palazzini M, Park MH, Tapson VF, Sitbon O. Treatment goals of pulmonary hypertension. J Am Coll Cardiol 2013; 62 Suppl: D73-81.
[26] Beghetti M, Tissot C. Pulmonary arterial hypertension and congenital heart disease: targeted therapies and operability. J Thorac Cardiovasc Surg 2009; 138: 785-786.
[27] Mohr FW, Seeburger J, Misfeld M. Keynote Lecture-Transmitral hypertrophic obstructive cardiomyopathy (HOCM) repair. Ann Cardiothorac Surg 2013; 2: 729-732.
[28] Joassard OR, Amirouche A, Gallot YS, Desgeorges MM, Castells J, Durieux AC, Berthon P, Freyssenet DG. Regulation of Akt-mTOR, ubiquitin-proteasome and autophagy-lysosome pathways in response to formoterol administration in rat skeletal muscle. Int J Biochem Cell Biol 2013; 45: 2444-2455.
[29] Anderson RH, Spicer DE, Giroud JM, Mohun TJ. Tetralogy of Fallot: nosological, morphological,

and morphogenetic considerations. Cardiol Young 2013; 23: 857-865.
[30] van de Veerdonk MC, Dusoswa SA, Tim Marcus J, Bogaard HJ, Spruijt O, Kind T, Westerhof N, Vonk-Noordegraaf A. The importance of trabecular hypertrophy in right ventricular adaptation to chronic pressure overload. Int J Cardiovasc Imaging 2014; 30: 357-65.
[31] McIlvennan CK, Allen LA. To DT or not to DT, that is the question: working toward a comprehensive, patient-centered perspective on left ventricular assist device for destination therapy. Circ Cardiovasc Qual Outcomes 2014; 7: 13-4.
[32] Kapur NK, Paruchuri V, Aronovitz MJ, Qiao X, Mackey EE, Daly GH, Ughreja K, Levine J, Blanton R, Hill NS, Karas RH. Biventricular remodeling in murine models of right ventricular pressure overload. PLoS One 2013; 8: e70802.
[33] Arsenault M, Zendaoui A, Roussel E, Drolet MC, Dhahri W, Grenier A, Gascon S, Sarrhini O, Rousseau JA, Lecomte R, Couet J. Angiotensin II-converting enzyme inhibition improves survival, ventricular remodeling, and myocardial energetics in experimental aortic regurgitation. Circ Heart Fail 2013; 6: 1021-1028.
[34] Drake JI, Bogaard HJ, Mizuno S, Clifton B, Xie B, Gao Y, Dumur CI, Fawcett P, Voelkel NF, Natarajan R. Molecular signature of a right heart failure program in chronic severe pulmonary hypertension. Am J Respir Cell Mol Biol 2011; 45: 1239-1247.
[35] Rothermund L, Lorenz M, Schnieber A, Eberson J, Bauhaus I, Bernhard Haug M, Schulz A, Keller F, Vetter R, Kreutz R. Impact of nephron number dosing on cardiorenal damage and effects of ACE inhibition. Am J Hypertens 2011; 4: 474-481.
[36] Sundstrom L, Greasley PJ, Engberg S, Wallander M, Ryberg E. Succinate receptor GPR91, a Gα(i) coupled receptor that increases intracellular calcium concentrations through PLCβ. FEBS Lett 2013; 587: 2399-2404.
[37] Zhang L, Jaswal JS, Ussher JR, Sankaralingam S, Wagg C, Zaugg M, Lopaschuk GD. Cardiac insulin-resistance and decreased mitochondrial energy production precede the development of systolic heart failure after pressure-overload hypertrophy. Circ Heart Fail 2013; 6: 1039-1048.
[38] Gartner F, Seidel T, Schulz U, Gummert J, Milting H. Desensitization and internalization of endothelin receptor A: impact of G protein-coupled receptor kinase 2 (GRK2)-mediated phosphorylation. J Biol Chem 2013; 288: 32138-32148.
[39] Sheth H, Gorey C, Roush N, Smallman S, Collantes E, Santoro M, Olson B, Fitzgerald L, Lee PH, Shen XJ. A Multiplexed Fluorescent Calcium and NFAT Reporter Gene Assay to Identify GPCR Agonists. Curr Chem Genomics Transl Med 2013; 7: 1-8.
[40] Andrews SP, Brown GA, Christopher JA. Structure-Based and Fragment-Based GPCR Drug Discovery. Med Chem 2014; 9: 256-75.
[41] Zhan X, Wang J, Liu Y, Peng Y, Tan W. GPCR-like signaling mediated by smoothened contributes to acquired chemoresistance through activating Gli. Mol Cancer 2014; 13: 4.
[42] Heinke J, Juschkat M, Charlet A, Mnich L, Helbing T, Bode C, Patterson C, Moser M. Antagonism and synergy between extracellular BMP modulators Tsg and BMPER balance blood vessel formation. J Cell Sci 2013; 126: 3082-3094.
[43] Banerjee P, Bandyopadhyay A. Cytosolic dynamics of annexin A6 triggers feedback regulation of hypertrophy via atrial natriuretic peptide in cardiomyocytes. J Biol Chem 2014; 289: 5371-85.
[44] Kolwicz SC Jr, Purohit S, Tian R. Cardiac metabolism and its interactions with contraction, growth, and survival of cardiomyocytes. Circ Res 2013; 113: 603-616.
[45] Lee H, Yoo YS, Lee D, Song EJ. Cholesterol induces cardiac hypertrophy by activating the AKT pathway. J Steroid Biochem Mol Biol 2013; 138: 307-313.
[46] Montano MM, Desjardins CL, Doughman YQ, Hsieh YH, Hu Y, Bensinger HM, Wang C, Stelzer JE, Dick TE, Hoit BD, Chandler MP, Yu X, Watanabe M. Inducible re-expression of HEXIM1 causes physiological cardiac hypertrophy in the adult mouse. Cardiovasc Res 2013; 99: 74-82.
[47] Vazquez-Medina JP, Popovich I, Thorwald MA, Viscarra JA, Rodriguez R, Sonanez-Organis JG, Lam L, Peti-Peterdi J, Nakano D, Nishiyama A, Ortiz RM. Angiotensin receptor-mediated oxidative stress is associated with impaired cardiac redox signaling and mitochondrial function in insulin-resistant rats. Am J Physiol Heart Circ Physiol 2013; 305: H599-607.
[48] Wang HX, Yang H, Han QY, Li N, Jiang X, Tian C, Du J, Li HH. NADPH oxidases mediate a cellular "memory" of angiotensin II stress in hypertensive cardiac hypertrophy. Free Radic Biol Med 2013; 65: 897-907.
[49] Cannavo A, Liccardo D, Koch WJ. Targeting cardiac β-adrenergic signaling via GRK2 inhibition for heart failure therapy. Front Physiol 2013; 4: 264.

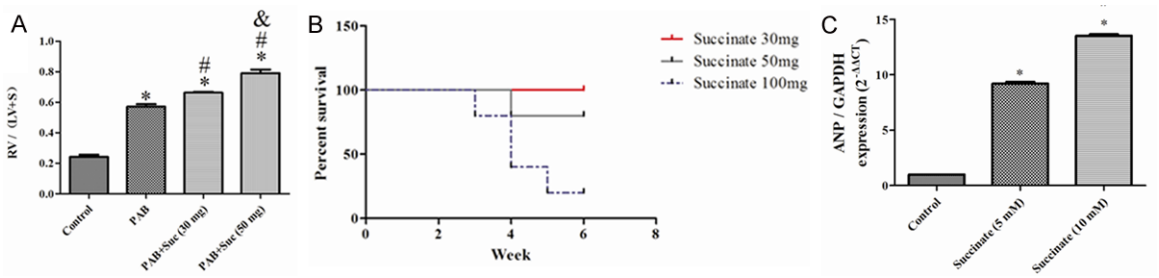

Appendix Figure 1. The succinate concentration in this article. A: RV hypertrophy indexed by the ratio of the wet weight of the RV to the left ventricular wall plus the septum [RV/(LV+S)] from the sham, PAB, PAB+succinate (30 mg) and PAB+succinate (50 mg) rats (n=4); *$P < 0.05$, compared with the sham; #$P < 0.05$, compared with the PAB rats; &$P < 0.05$, compared with the PAB+succinate rats (30 mg); B: The percent survival in the PAB+succinate (30 mg), PAB+succinate (50 mg) and PAB+succinate (100 mg) rats (n=5); C: *Anp* gene expression in the sham, succinate (5 mM) and succinate (10 mM) groups (n=5); *$P < 0.05$, compared with the sham; #$P < 0.05$, compared with the succinate (5 mM) group.

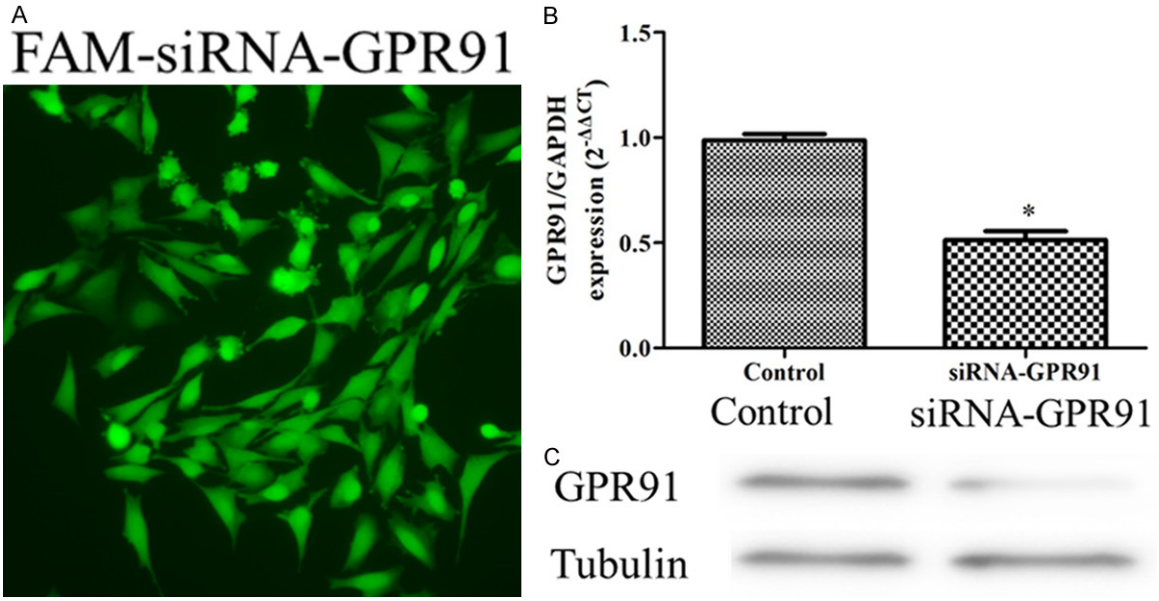

Appendix Figure 2. Small interfering RNA (siRNA) transfection. A: Immunofluorescent images of cardiomyocytes with fluorescein isothiocyanate (FITC)-conjugated -siRNA GPR91; B: GPR91 gene expression in the control, siRNA-GPR91 group (n-3); C: GPR91 protein expression in the control, siRNA-GPR91 group (n-3).